Final Report

Physics of Complex Networks: Structure and Dynamics

Università degli Studi di Padova

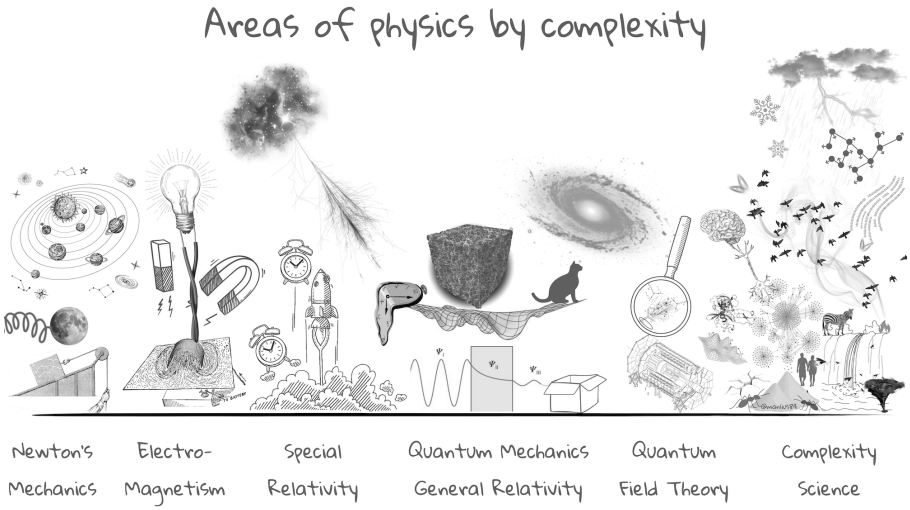

Project # X: ....

Aquistapace Tagua, Franco

Last update: February 11, 2025

Contents

1 | Song-Havlin-Makse self-similar model

1.1 | Introduction and methods

The work by Song, Havlin and Makse [6] aims to explain the characteristic features of empirical scale–free fractal and non–fractal networks by means of a single growth model, that has the concept of renormalisation at its core. More specifically, the proposed growth mechanism works as the inverse of the renormalisation procedure. The goal of this task is then to reproduce the growth and renormalisation procedures, and to recover the characteristic behaviour of fractal and non–fractal networks through relevant descriptors.

When performing the growth process of a network, each existing node is considered as a future hub. For a node with degree k, mk offspring nodes are attached to it at each growth step. Then, each edge between two of the original nodes is removed with probability $p = 1 - e$, and replaced by an edge between two of their offspring. The parameter e then controls the hub–hub attraction/repulsion behaviour of the network. Mode I growth, given by $e \to 1$, leads to hub–hub attraction and a non–fractal topology. Meanwhile, Mode II growth, given by $e \to 0$, leads to hub–hub repulsion and a fractal network. This growth process is referred to as the minimal model. The renormalisation of a network is then done as described in the source material, by covering its N nodes with $N_B(L_B)$ boxes, where the maximum shortest path between any two nodes in a box must be L_B.

For each case $e = 1.0, 0.8$, a set of 10 graphs is generated with the minimal model. In all cases, the network is initialised as a star graph with $N_{init} = 5$ nodes. Then, the growth mechanism is applied $n_{growth} = 4$ times, with a growth factor of $m = 2$. Once obtained, each graph is then subjected to the normalisation procedure for distances $1 \leq L_B \leq 32$. Furthermore, for each minimal model graph an uncorrelated version is generated by random swapping of links, while maintaining the degree distribution. Additional details on the methodology can be found in section 4.1 of the Supplementary Material.

1.2 | Results and discussion

The correlation profile, $R(k_1, k_2)$, can be used to visualise the correlated topological structure of the minimal model, in comparison to its random uncorrelated counterpart.

Fig. 1.1 presents the $R(k_1, k_2)$ matrices for both cases $e = 1.0, 0.8$. It can be seen that $e = 1.0$ leads to hub–hub attraction, while hub–hub repulsion is observed for the case $e = 0.8$. This descriptor is however insufficient to define the fractality of a network, as it cannot describe how the topology of the network changes under renormalisation.

In order to complement this, the scaling relations $N_B(L_B)/N$ and $\mathcal{S}(L_B)$ are estimated for the minimal model graphs, where $\mathcal{S}(L_B)$ is the maximum degree scaling. The results of $N_B(L_B)/N$ and $\mathcal{S}(L_B)$ are presented in Fig. 1.2 with respect to L_B, for both cases $e = 1.0, 0.8$. As in the source material, an exponential decrease of both descriptors can be seen for the non–fractal topology resulting from the case $e = 1.0$. Meanwhile, the power–law behaviour of fractal networks is observed in both descriptors for the case $e = 0.8$. A finite–size effect can be observed for large values of L_B, more noticeably for the case $e = 1.0$, which appears as a constant value of the scaling relations.

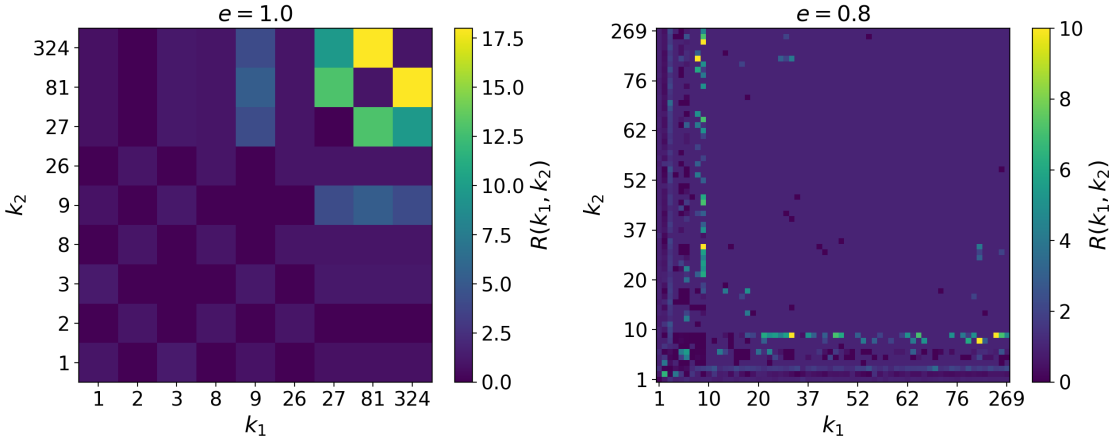

Figure 1.1: Correlation profile $R(k_1, k_2)$ of networks generated with the minimal model, for the cases $e = 1.0$ (left) and $e = 0.8$ (right).

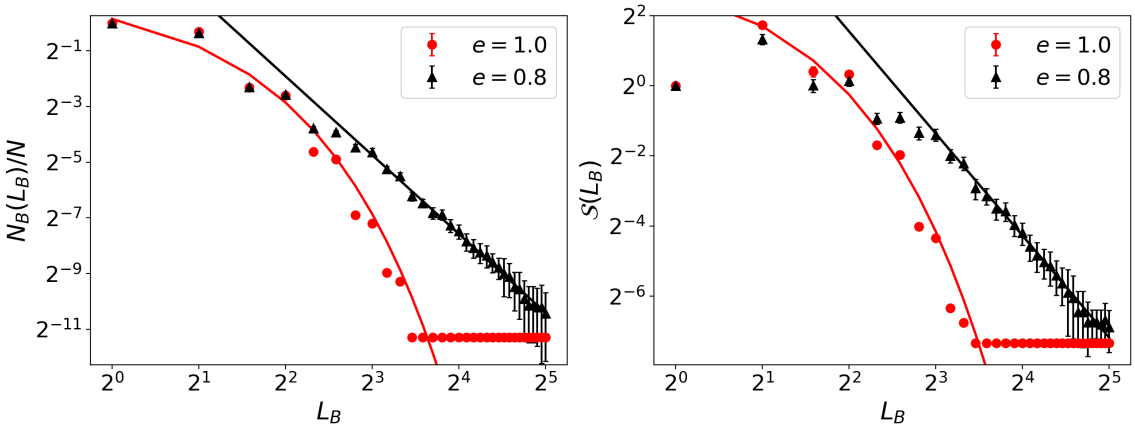

Figure 1.2: Scaling relations $N_B(L_B)/N$ (left) and $\mathcal{S}(L_B)$ (right) with respect to box distance L_B. Results are shown for networks generated with the minimal model, for the cases $e = 1.0$ and $e = 0.8$. The fitted theoretical models are shown as solid lines.

2 | Sandpile dynamics on complex networks

2.1 | Introduction and methods

The aim of this task is to study the behaviour of the Bak-Tang-Wiesenfeld sandpile model (BTW) [2] on complex networks, and to reproduce the main findings presented by Bonabeau [3], Goh et al. [5] and Brummitt et al. [4]. The BTW can be used to model the phenomenon of failure cascades observed in many real–world networks, and can thus aid in understanding the relationship between the architecture of a network and its robustness in the face of node failures. The first part of the task focuses on scale–free networks, where the power–law behaviour of failure cascades depends on the degree distribution. The second part focuses on interdependent networks, where the interconnection between systems can either mitigate or exacerbate failure cascades.

The BTW is simulated here as follows: at each time step, a grain is added to a random node i of the system. If the grains at any node i exceed its degree k_i, then it becomes unstable and topples one grain to each neighbour, and an avalanche is considered to begin. For each toppled grain, there is a probability f that the grain is lost, which helps avoid the overloading of the system. Then, each node is checked again for instability and the toppling is repeated in parallel until there are no more unstable nodes, and the avalanche is considered as finished. This process is repeated until a certain amount of avalanches are registered, or until a fixed amount of grains have been added to the system. Avalanches with no lost grains are termed *bulk* avalanches.

Simulations are first performed on scale–free networks with degree exponents $\gamma \in (2, \infty)$ and $f = 10^{-3}$. The simulations are finished after 10^6 avalanches have been observed, and only bulk avalanches are considered for analysis. Additionally, simulations are performed on interdependent networks linked with uncorrelated Bernoulli couplings of probability $p \in [0.001, 0.5]$, with $f = 10^{-2}$. These simulations are finished after 2×10^5 grains are added to the system. Additional details on the methodology can be found in section 4.2 of the Supplementary Material.

2.2 | Results and discussion

In general, the area of a bulk avalanche, A, is expected to be distributed as $p_a(A) \sim A^{-\tau} \exp(-A/s_c)$, where $s_c \sim (\langle k \rangle f)^{-1}$ is the avalanche characteristic size. Additionally, the dynamic exponent z characterises the relationship between the avalanche size, S,

and its duration, T, as $S \sim T^z$. From a branching process approach, these exponents are expected to depend on the degree distribution exponent γ as $\tau = \gamma/(\gamma-1)$ and $z = (\gamma-1)/(\gamma-2)$ for $\gamma \in (2,3)$, and to have values $\tau = 3/2$ and $z = 2$ for $\gamma > 3$. Fig. 2.1 presents the exponents τ and z with respect to γ, obtained from the simulations on scale–free networks. The observed behaviour qualitatively agrees with the theoretical prediction, and the quantitative disagreement may be due to the finite size effect.

For interdependent networks, increasing the Bernoulli link probability p between subsystems can help mitigate large avalanches up to a point, p^*. Fig. 2.2 presents the probability of a large avalanche $P(S_{large})$ with respect to p, considering both the local and inflicted avalanche size, as well as the global average. From the simulation results, the optimal link probability is $p^* \approx 0.075$, in agreement with the source material [4].

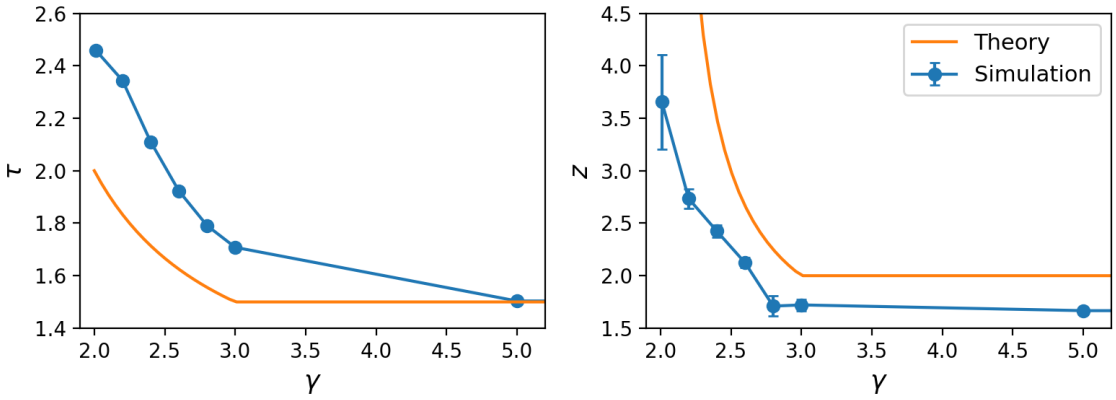

Figure 2.1: Avalanche area distribution exponent, τ, (left) and dynamic exponent, z, (right) with respect to the degree distribution exponent, γ, of scale–free networks. The best fit from simulations is presented, alongside the theoretical prediction.

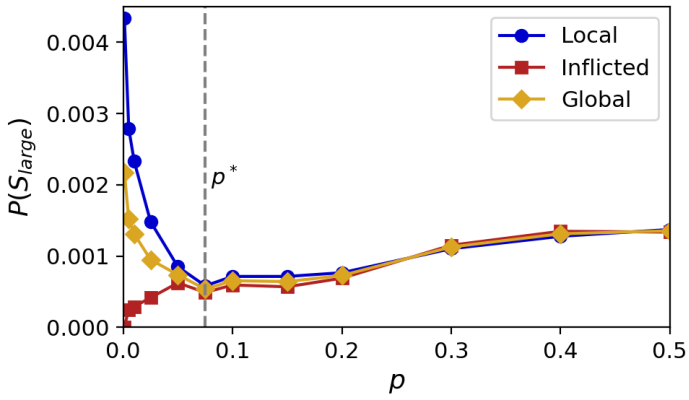

Figure 2.2: Probability of a large avalanche, $P(S_{large})$, with respect to the link probability, p, for interdependent networks connected through uncorrelated Bernoulli coupling. The results for local, inflicted and global avalanches are shown, as well as the critical point p^*.

3 | Data analytics of public transport networks

3.1 | Introduction and methods

The Citylines platform is a collaborative effort to map the public transport systems of the world [1]. It offers a dataset that contains a detailed history of the development of transport networks in several cities, from multiple countries. The aim of this task is to reconstruct the transport networks from the available data, and to perform an analysis of such networks. The first part of the task is concerned with the development of the methods and heuristics that are necessary to reconstruct and infer networks from the geographical location of nodes and edges. Each network is built as a set of connected components, where each connected component represents a public transport line, in which the nodes represent stations and edges are a simplified representation of the sections connecting the stations. The second part of the task is concerned with the analysis and characterisation of the produced networks, by means of standard topological descriptors.

The construction of the transport network for a given city is done by iterating the same procedure for all available transport lines. First, all stations that are linked to the line are stored as nodes. Then, the edges between the nodes are built in a three–step process. Initially, each node attempts to connect to its two closest neighbours, using their geographical location as position. The connection is accepted unless the neighbours are closer to each other than to the reference node, in which case the edge is only added between the reference node and its closest neighbour. Then, for every section of the line, an edge between the two nodes that are closest to the respective ends is attempted. In this case, the edge is rejected if there already exists a path between the nodes. Finally, a rewiring step is performed to avoid spurious edges: for each two connected nodes, if a shorter edge between one of the nodes and a neighbour is possible then the original edge is replaced by the shorter alternative. This rewiring is repeated until no more replacements are possible. A check is performed throughout the entire process so that the same edge is not built multiple times.

The analysis and characterisation of the transport networks is done by means of topological descriptors. To take into account any possible relationship between topology and size, the networks are classified into small ($N < 100$), medium ($100 \leq N < 500$) and large ($N \geq 500$) according to the amount of nodes N. Additional details on the methodology can be found in section 4.3 of the Supplementary Material.

3.2 | Results and discussion

Fig. 3.1 presents the degree distribution of small, medium and large cities. It can be noted that the distribution does not change significantly between different city sizes. The large ratio between $P(k = 2)$ and $P(k = 1)$ may indicate that transport networks consist of few lines composed of many stations. In particular, this appears to be less notable for small cities. Additionally, the low proportion of nodes with $k = 3, 4$ points towards transport lines having a low amount of branches.

The average shortest path length, I_G, is shown in Fig. 3.2 as a function of the number of nodes N, both for the largest connected component (LCC) and as an average over all connected components. For the LCC, the shortest path appears to scale as $I_G \propto \log(N)$, while for the average over all connected components it seems to scale as $I_G \propto \sqrt{\log(N)}$.

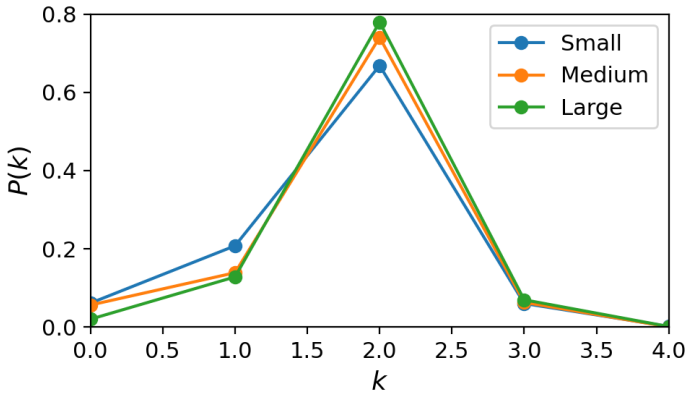

Figure 3.1: Degree distribution, $P(k)$, for city transport networks. Results are shown for small, medium and large cities.

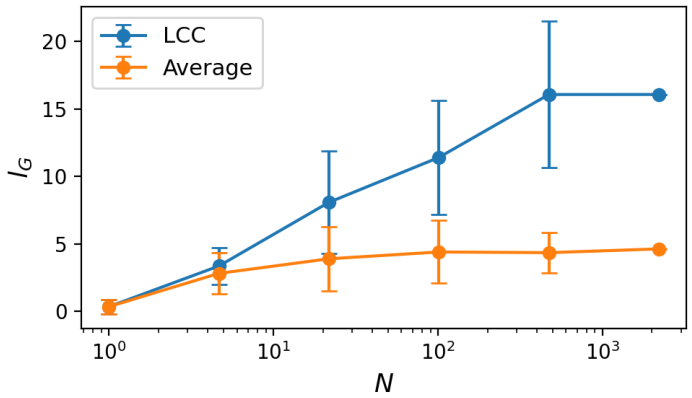

Figure 3.2: Average shortest path length, I_G, with respect to the number of nodes, N, for city transport networks. The results are presented for the largest connected component of the network (LCC), as well as for the average over all connected components.

4 | Supplementary material

4.1 | Song-Havlin-Makse self-similar model

Algorithmic implementation of the renormalisation procedure

The renormalisation of a given network is performed algorithmically as follows:

1. Initialise a box with a randomly picked node.
2. For every remaining node i, add it to the box if $\max_{j \in B} d(i,j) \leq L_B$, where B contains the nodes currently in the box, and $d(i,j)$ is the shortest path between nodes i and j.
3. Repeat steps 1. and 2. with the remaining available nodes until all nodes are assigned to a box.

Correlation profiles

The correlation profile $R(k_1, k_2) = P(k_1, k_2)/P_r(k_1, k_2)$ is defined as the ratio between the joint degree–degree probability distribution of the network of interest, $P(k_1, k_2)$, and the joint degree–degree probability distribution of a randomised uncorrelated version of the same network, $P_r(k_1, k_2)$, where the links have been randomly rewired while preserving the degree distribution.

In this work, the joint degree–degree probability distribution is estimated in a frequentist approach, by considering all equivalent instances as observations. For example, to obtain $P(k_1, k_2)$ for the minimal model graph with $e = 1.0$, the degree–degree pairs of the 10 graphs generated for $e = 1.0$ are collected. Then, the joint probability for a given pair (k_1, k_2) is calculated as in Eq. 4.1:

$$P(k_1, k_2) = \frac{N_{obs}(k_1, k_2)}{N_{obs,tot}} \quad , \tag{4.1}$$

where $N_{obs}(k_1, k_2)$ is the number of occurrences of the pair (k_1, k_2), and $N_{obs,tot}$ is the total number of observations. The same methodology is applied for the calculation of $P_r(k_1, k_2)$. No interpolation is done for pairs (k_1', k_2') that are not observed, and their probability is thus taken as $P(k_1', k_2') = 0$.

Scaling relations

The descriptor $N_B(L_B)/N$ is defined as the ratio between the number of original nodes, N, and the number of boxes, N_B, obtained after performing a renormalisation step with box size L_B. Meanwhile, the descriptor $\mathcal{S}(L_B) = k_B(L_B)/k_{hub}$ is the ratio between the maximum degree of the boxes after a renormalisation step with box size L_B, $k_B(L_B)$, and the maximum degree of the among the original nodes, k_{hub}. For both scaling relations, $N_B(L_B)/N$ and $\mathcal{S}(L_B)$, the mean value and standard deviation is obtained for each L_B from the 10 networks generated for both cases $e = 1.0, 0.8$. From the obtained results, the theoretical models proposed in the source material [6] are fitted.

For the fractal case $e = 0.8$, $N_B(L_B)/N$ and $\mathcal{S}(L_B)$ are described, respectively, by Eqs. 4.2 and 4.3:

$$N_B(L_B)/N = C_N(L_B + L_0)^{-d_B} \tag{4.2}$$

$$\mathcal{S}(L_B) = C_S(L_B + L_0)^{-d_k} \tag{4.3}$$

where L_0, d_B, d_k, C_N and C_S are parameters fitted from the data. The data points with $L_B < 8$ were excluded from the fit of $N_B(L_B)/N$, and those with $L_B < 12$ were excluded from the fit of $\mathcal{S}(L_B)$. From the fit, the values $d_B = 2.83$ and $d_k = 2.91$ are obtained.

On the other hand, for the non–fractal case $e = 1.0$, $N_B(L_B)/N$ and $\mathcal{S}(L_B)$ are described, respectively, by Eqs. 4.4 and 4.5:

$$N_B(L_B)/N = C_N \exp(-L_B/L_0) \tag{4.4}$$

$$\mathcal{S}(L_B) = C_S \exp(-L_B/L_0) \tag{4.5}$$

where again L_0, C_N and C_S are fitted from the data. In this case, the data points with $L_B > 12$ are excluded from the fit of both $N_B(L_B)/N$ and $\mathcal{S}(L_B)$.

4.2 | Sandpile dynamics on complex networks

Bak-Tang-Wiesenfeld sandpile model simulations

In general, for each avalanche event in the Bak-Tang-Wiesenfeld model simulations, the following quantities are registered:

- Avalanche area, A: defined as the number of distinct nodes participating in an avalanche event.
- Avalanche size, S: defined as the number of toppling events in a given avalanche.
- Number of toppled grains, G.
- Avalanche duration, T.

- Bulk avalanche status, B: defined as a boolean value that indicates if no grains are lost during the avalanche.

For the simulations on interdependent networks the following observations are additionally registered: subgraph where an avalanche originates, local size of the avalanche in the origin subgraph and inflicted size of the avalanche on the non-origin subgraph.

Generation of scale–free networks

In this work, the static model from [5] is used to generate scale–free networks with desired properties as follows. First, a set of N nodes are indexed as $i = 1, ..., N$ and are assigned a weight $w_i = i^{-\alpha}$, where $\alpha \in [0, 1)$ controls the degree distribution of the network as $\gamma = 1+1/\alpha$, for large N. Then, in an iterative manner, two nodes i and j are selected with relative probabilities w_i and w_j, and an edge is created between them if no edge is already present. This process is repeated until the average degree of the network is $\langle k \rangle = 2m$. Here, the networks are generated with 2×10^5 nodes, $m = 2$ leading to an average degree $\langle k \rangle = 4$, and degree exponents $\gamma = 2.01, 2.2, 2.4, 2.6, 2.8, 3.0, 5.0, \infty$.

In order to avoid spurious effects in the sandpile simulations, isolated nodes and possibly other small subgraphs are removed from the system by only keeping the largest connected component. In general, the amount of removed nodes is not significant when compared to the size of the remaining network.

Characterisation of avalanches in scale–free networks

The distribution of the area of bulk avalanches in the simulations performed on scale–free networks, $P_a(A)$, is modelled here by Eq. 4.6:

$$P_a(A) = CA^{-\tau} \exp(-A/s_c) \ , \tag{4.6}$$

where C and τ are fitted from the data, and the avalanche characteristic size is set as $s_c = (\langle k \rangle f)^{-1}$. In order to fit the model, the observations for A are first binned logarithmically using $N_{bins} = 13$ bins, and the first $N_{skip} = 3$ bins are excluded from the fit. It is noted in this work that the choice of N_{bins} and N_{skip} has a significant impact on the resulting values for τ, and the results presented here are the ones closest to the theoretical prediction from the branching process approach.

On the other hand, the relationship between the bulk avalanche size S and the duration T is defined by Eq. 4.7:

$$S = C_z T^z \ , \tag{4.7}$$

where C_z and z are fitted from the data. To fit Eq. 4.7, the data outside of a range (T_{min}, T_{max}) is discarded. The values T_{min} and T_{max} are chosen so as to isolate the range in T where the model holds.

Fig. 4.1 presents $P_a(A)$ with respect to A, and S with respect to T for the bulk avalanches registered in simulations on the scale–free networks. The results are

presented for the cases $\gamma = 2.01, 2.2, 3.0, \infty$. The best fits of Eqs. 4.6 and 4.7, respectively, are also shown. The simulation results for $P_a(A)$ are presented after logarithmic binning, and only the mean values of S for each unique value of T are shown.

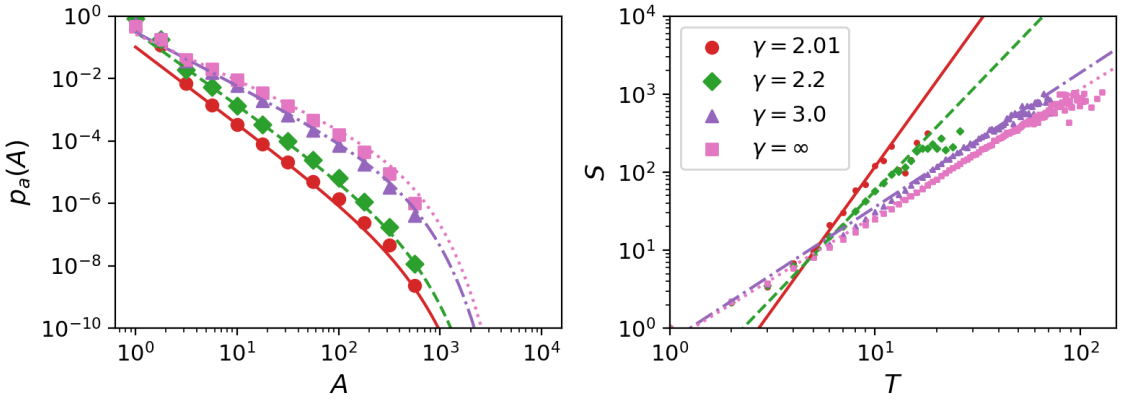

Figure 4.1: Distribution of avalanche area, $P_a(A)$, (left) and avalanche size, S, with respect to duration, T, (right) for bulk avalanches. The results for simulations on scale–free networks with degree exponent $\gamma = 2.01, 2.2, 3.0, \infty$ are shown, as well as the best fit of the theoretical models. To increase clarity, only the mean value of S for each unique value of T is shown for each case, and the marker size for data points (S, T) is reduced.

Generation of interdependent regular networks

In this work, each interdependent network is first initialised as two separate z-regular subgraphs, G_A and G_B, with uniform degree $z = 3$ and 2×10^3 nodes each. Then, the connection between these subgraphs is done by means of uncorrelated Bernoulli coupling, as follows: for each node in G_A a random number is uniformly sampled from $(0, 1)$, if that number is smaller than a threshold p then an available node from G_B is uniformly sampled and a link to it is established. The selected node from G_B is then removed from the set of available nodes, so that each node in G_A can be connected at most to a single node from G_B, and vice versa. In order to cover a wide but detailed range of p, a network is generated for each value in $p = 0.001, 0.005, 0.01, 0.025, 0.05, 0.075, 0.1, 0.15, 0.2, 0.3, 0.4, 0.5$.

Characterisation of avalanches in interdependent networks

A large avalanche is here defined as an avalanche with size $S > N'/2$, where N' is the amount of nodes in a single subgraph of the system. Additionally, the quantity $N_X^Y(S_{large})$ is defined as the amount of large avalanches measured in Y which originated in X, where $X, Y \in \{A, B\}$. Then, the probability of a large local avalanche, $P_{local}(S_{large})$, is defined by Eq. 4.8:

$$P_{local}(S_{large}) = \frac{1}{2}\left(\frac{N_A^A(S_{large})}{N^A} + \frac{N_B^B(S_{large})}{N^B}\right) , \tag{4.8}$$

where N^A and N^B are the total number of avalanches observed in A and B, respectively, regardless of their origin. On the other hand, the probability of a large inflicted avalanche, $P_{inf}(S_{large})$, is defined as in Eq. 4.9:

$$P_{inf}(S_{large}) = \frac{1}{2}\left(\frac{N_A^B(S_{large})}{N^B} + \frac{N_B^A(S_{large})}{N^A}\right) . \tag{4.9}$$

Finally, the global probability of a large avalanche, $P_{global}(S_{large})$, is defined by Eq. 4.10:

$$P_{global}(S_{large}) = \frac{P_{local}(S_{large}) + P_{inf}(S_{large})}{2} . \tag{4.10}$$

Another relevant factor when considering interconnected systems is the size of the largest avalanches in the entire network. In this work, it is noted that such size is directly related to the coupling probability p. This is displayed in Fig. 4.2 as a rank plot of the size S for the 10^3 largest avalanches, for $p = 0.001, 0.01, 0.1$. It can be seen that an increase in p leads to an increase S for the largest avalanches in the system, in agreement to what is reported in the reference material [4].

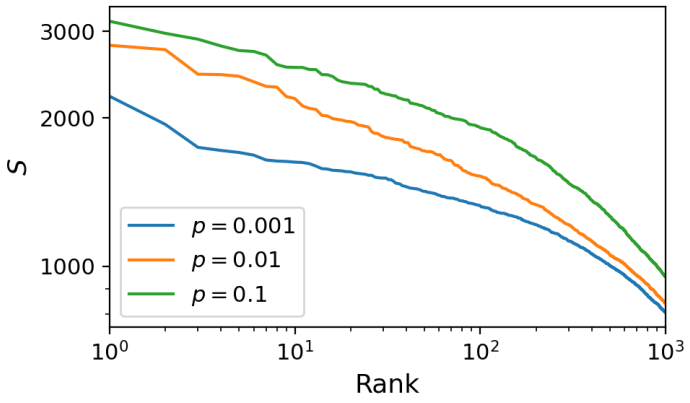

Figure 4.2: Rank plot of the avalanche size, S, for the 10^3 largest avalanches in interdependent networks. Results are presented for the cases $p = 0.001, 0.01, 0.1$.

4.3 | Data analytics of public transport networks

Description of the Citylines dataset

The totality of the data contained in the Citylines platform is distributed into separate files that contain the following information:

- Cities: Basic information about each city, including its name, location, identifier (ID) and name of the country.
- Systems: Name and ID of each transport system, as well as the city ID.

- Lines: Name and ID of each line, as well as the IDs of the corresponding city, system and transport mode.
- Sections: Geographical locations, historical data, length and ID for each section of each line, as well as the corresponding city ID.
- Section lines: Connects every section to its corresponding line by means of their respective IDs.
- Stations: Geographical location, historical data, name and ID of each station, as well as the corresponding city ID.
- Station lines: Connects every station to its corresponding line through their respective IDs.
- Transport modes: Name and ID of each transport mode.

Fig. 4.3 displays a network representation of the Citylines dataset files, with one possible way to link them. The edges may represent a one–to–one or a one–to–many mapping.

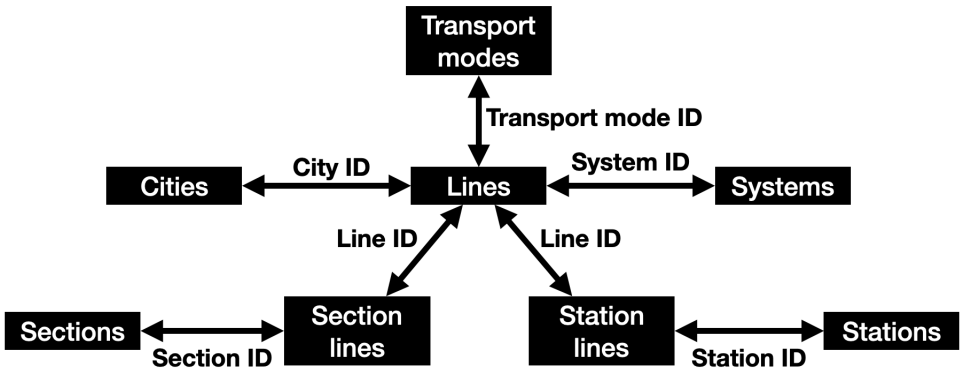

Figure 4.3: Network representation of the Citylines dataset. Each node represents a file, and the edges that are shown display one possible way to link the different files as one–to–one or one–to–many mappings.

Generation of transport networks from data

As described in the main text, the edges of each transport network are built using a set of criteria, which are motivated by the following reasoning:

- The first two edges attempted from every node to its closest neighbours are based on the assumption that stations belonging to the same line which are spatially close are likely to be connected.
- Since there is no data available to match line sections to specific stations, the spatial proximity of the stations to the section endpoints is used instead to infer such mapping.
- The edge rewiring process is based on the assumption that transport lines are built in an optimised fashion, where the different sections of the line are connected

by means of their closest stations.

As an example of the obtained results, Fig. 4.4 presents the generated networks for the cities of Tokyo and Seoul, where each color represents a transport mode.

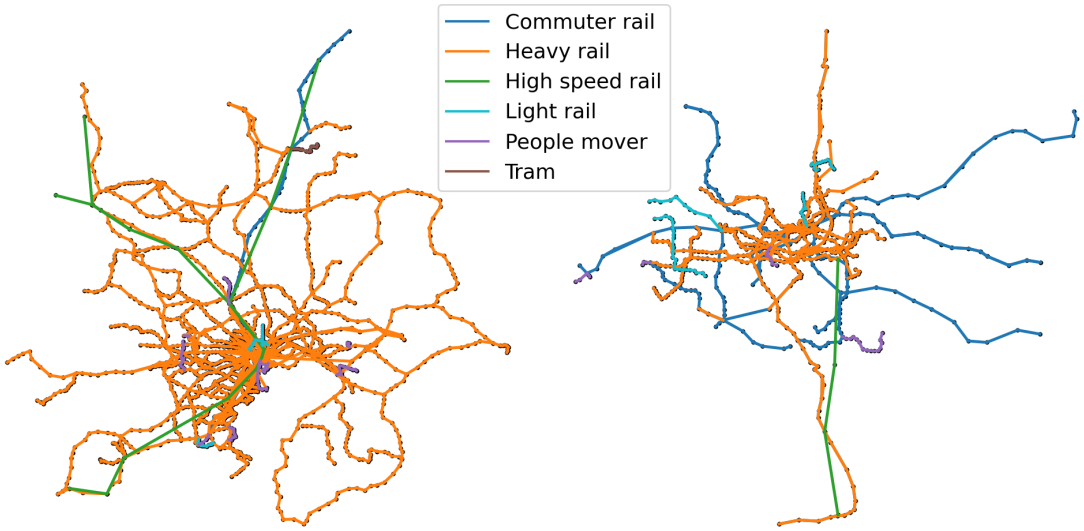

Figure 4.4: Transport networks for the cities of Tokyo (left) and Seoul (right), generated from the Citylines dataset. Nodes, representing stations, are displayed as dots at their geographical location, while edges are shown as lines and colored according to the corresponding transport mode.

For each city in the dataset, the respective transport network is saved as two files, one with node attributes and one with edge attributes. For the nodes, the stored information consists of a unique ID, the name of the station, its geographical location, the corresponding transport mode and its opening year. For the edges, on the other hand, the stored information consists of the IDs of the associated nodes, the transport mode, the name of the line and its opening year. The opening year of an edge is inferred as the opening year of the closest line section, and as the maximum between the opening years of the connected stations if section data is unavailable. Whenever the available data is not sufficient to reconstruct the network of a given city, the node and edge files are stored empty.

Topological characterisation of transport networks

All topological descriptors are estimated either with respect to the size of the network, given by the number of nodes N, or its discrete size classification as small, medium or large. Fig. 4.5 presents a histogram with the distribution of N for all the generated networks. After applying the size criteria presented in the main text, a total of 64 small cities, 42 medium cities and 9 large cities are obtained.

The degree distribution $P_S(k)$ for a given city size S is estimated in a frequentist approach as in Eq. 4.11:

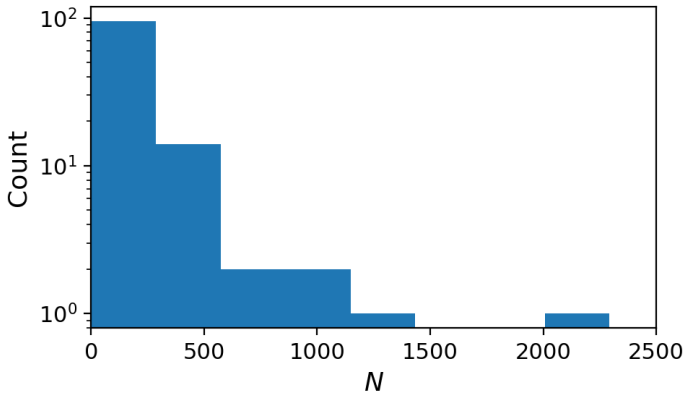

Figure 4.5: Histogram of the number of nodes, N, for the transport networks generated from the Citylines dataset.

$$P_S(k) = \frac{N_S(k)}{\sum_{k'} N_S(k')} \quad , \tag{4.11}$$

where $S \in \{Small, Medium, Large\}$ and $N_S(k)$ is the number of nodes with degree k accumulated over all networks in class S.

Additionally, the average shortest path length I_G is defined for a connected component G by Eq. 4.12:

$$I_G = \frac{1}{N_G(N_G - 1)} \sum_{i \neq j} d(\nu_i, \nu_j) \quad , \tag{4.12}$$

where N_G is the number of nodes, each ν_i is a node in G and $d(\nu_i, \nu_j)$ is the distance, or the length of the shortest path, between nodes ν_i and ν_j.

5 | Bibliography

[1] Citylines dataset. https://www.citylines.co/data. Accessed: 2025-01-28.

[2] Per Bak, Chao Tang, and Kurt Wiesenfeld. Self-organized criticality: An explanation of the 1/f noise. *Physical review letters*, 59(4):381, 1987.

[3] Eric Bonabeau. Sandpile dynamics on random graphs. *Journal of the Physical Society of Japan*, 64(1):327–328, 1995.

[4] Charles D Brummitt, Raissa M D'Souza, and Elizabeth A Leicht. Suppressing cascades of load in interdependent networks. *Proceedings of the national academy of sciences*, 109(12):E680–E689, 2012.

[5] K-I Goh, D-S Lee, B Kahng, and D Kim. Sandpile on scale-free networks. *Physical review letters*, 91(14):148701, 2003.

[6] Chaoming Song, Shlomo Havlin, and Hernán A Makse. Origins of fractality in the growth of complex networks. *Nature physics*, 2(4):275–281, 2006.